iScience, Volume *23*

Supplemental Information

PTPσ Controls Presynaptic Organization of Neurotransmitter Release Machinery at Excitatory Synapses

Kyung Ah Han, Hee-Yoon Lee, Dongseok Lim, Jungsu Shin, Taek Han Yoon, Chooungku Lee, Jeong-Seop Rhee, Xinran Liu, Ji Won Um, Se-Young Choi, and Jaewon Ko

SUPPLEMENTAL FIGURES

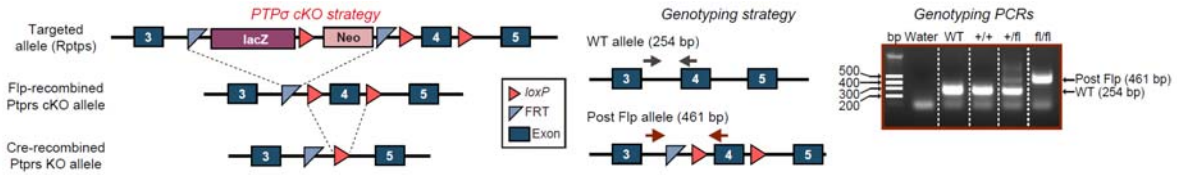

Supplemental Figure S1. Generation of PTPσ floxed Mice. Related to *All Figures*.

Conditional KO (cKO) strategy for PTPσ mouse lines. Exon 4 of the PTPσ gene was targeted (left). Primer locations for the WT and post Flp alleles are indicated with arrows (middle). PCR genotyping of WT and PTPσ floxed mice (right).

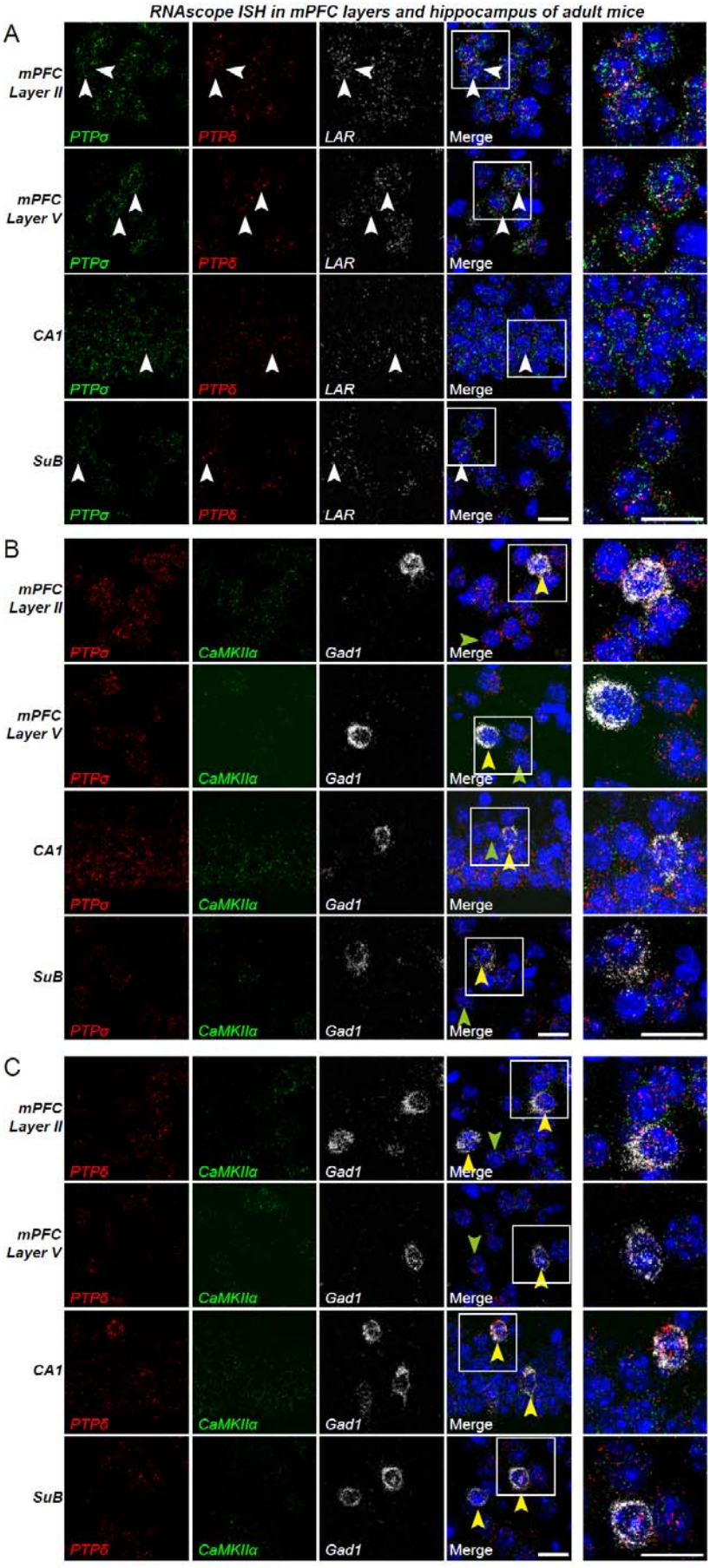
RNAscope ISH in mPFC layers and hippocampus of adult mice
A
mPFC Layer II
mPFC Layer V
CA1
SuB
PTPσ
PTPδ
LAR
Merge
B
CaMKIIα
Gad1
C

Supplemental Figure S2. Detection of LAR-RPTP mRNAs in Both Glutamatergic and GABAergic Neurons of Adult Mouse Brain. Related to *All Figures.*

(**A**) Representative high-resolution image of adult mouse brain regions (PFC layer II, mPFC layer V, hippocampal CA1, and SuB) visualized with probes targeting PTPσ (green), PTPδ (red) and LAR (white), and counterstained with DAPI (blue). White arrows indicate neurons with single cells expressing PTPσ, PTPδ and LAR mRNAs. Images (boxed in the merged image) on the right side are enlarged to clearly show quadruple labeling at the single-cell level. Scale bar, 20 μm.

(**B**) Representative high-resolution image of the indicated mouse brain regions, showing expression of PTPσ (red) in CaMKIIα-positive pyramidal neurons (green) and Gad1-positive GABAergic interneurons (white). Images (boxed in the merged image) on the right side are enlarged to clearly show quadruple labeling at the single-cell level. Scale bar, 20 μm.

(**C**) Representative high-resolution image of the indicated mouse brain region, showing expression of PTPδ (red) in CaMKIIα-positive pyramidal neurons (green) and Gad1-positive GABAergic interneurons (white). Images (boxed in the merged image) on the right side are enlarged to clearly show quadruple labeling at the single-cell level. Scale bar, 20 μm.

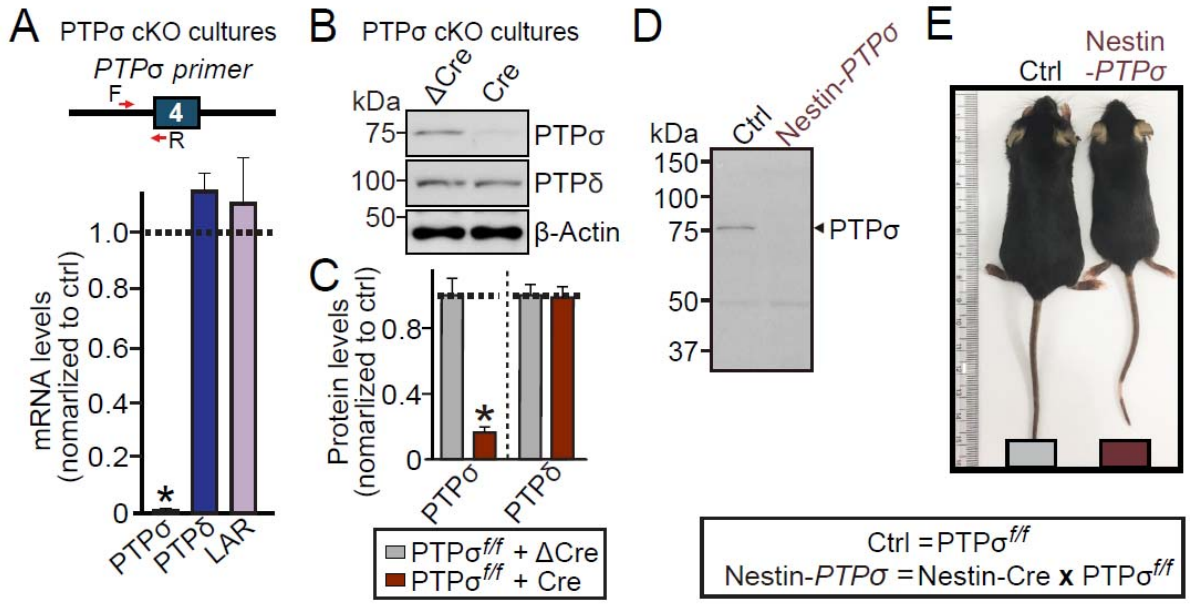

Supplemental Figure S3. Validation of PTPσ cKO Mice. Related to *All Figures*.

(**A**) Quantitative RT-PCR analysis of neuron RNA. Relative levels of PTPσ, PTPδ, and LAR mRNAs were measured in cultured cortical neurons infected with lentiviruses expressing Cre-recombinase. Data are means ± SEMs (n = 4 independent experiments).

(**B and C**) Representative immunoblot image (**B**) and quantitative analysis (**C**) of PTPσ protein in cultured cortical neurons infected with lentiviruses expressing Cre recombinase. β-actin was used as a loading control. Data are means ± SEMs (n = 4 independent experiments).

(**D**) Representative immunoblot analysis of level of PTPσ protein in brain homogenates from 8-week old control and PTPσ cKO mice. Levels of PTPσ protein was measured in the PTPσ floxed mice crossed with *Nestin-Cre* mice (Nestin-*PTPσ*) or respective PTP floxed mice (Ctrl). Arrows indicate band(s) immunoreactive with PTPσ-specific antibody.

(**E**) Images illustrating the body size of littermate control (Ctrl), Nestin-*PTPσ* mouse at 2 months of age. Nestin-*PTPσ* mouse was significantly smaller than age- and sex-matched Ctrl mice.

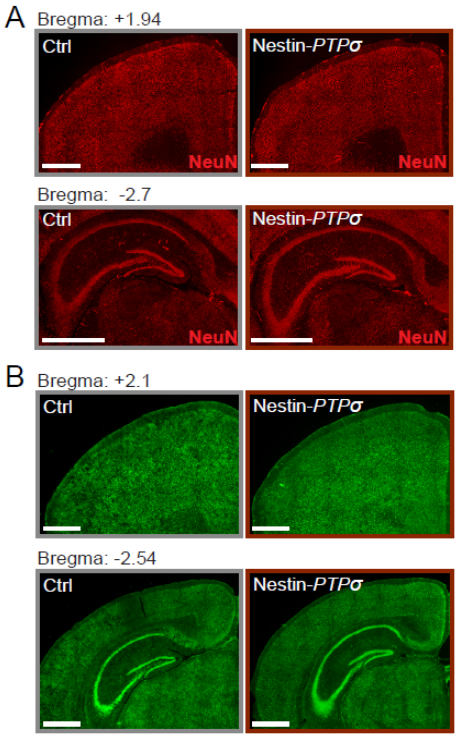

Supplemental Figure S4. Intact Cytoarchitecture in Conditional PTPσ KO Mice. Related to *All Figures.*

(**A**) Representative images of NeuN staining. Brain sections from *PTPσ*$^{f/f}$ (Ctrl) and Nestin-PTPσ mice were stained with the neuronal marker NeuN (red). Scale bar: 1 mm.

(**B**) Representative images of Nissl staining. Brain sections from *PTPσ*$^{f/f}$ (Ctrl) mice and from Nestin-PTPσ mice stained with NeuroTrace™ 500/525 Green Fluorescent Nissl Stain solution (green). Scale bar: 1 mm.

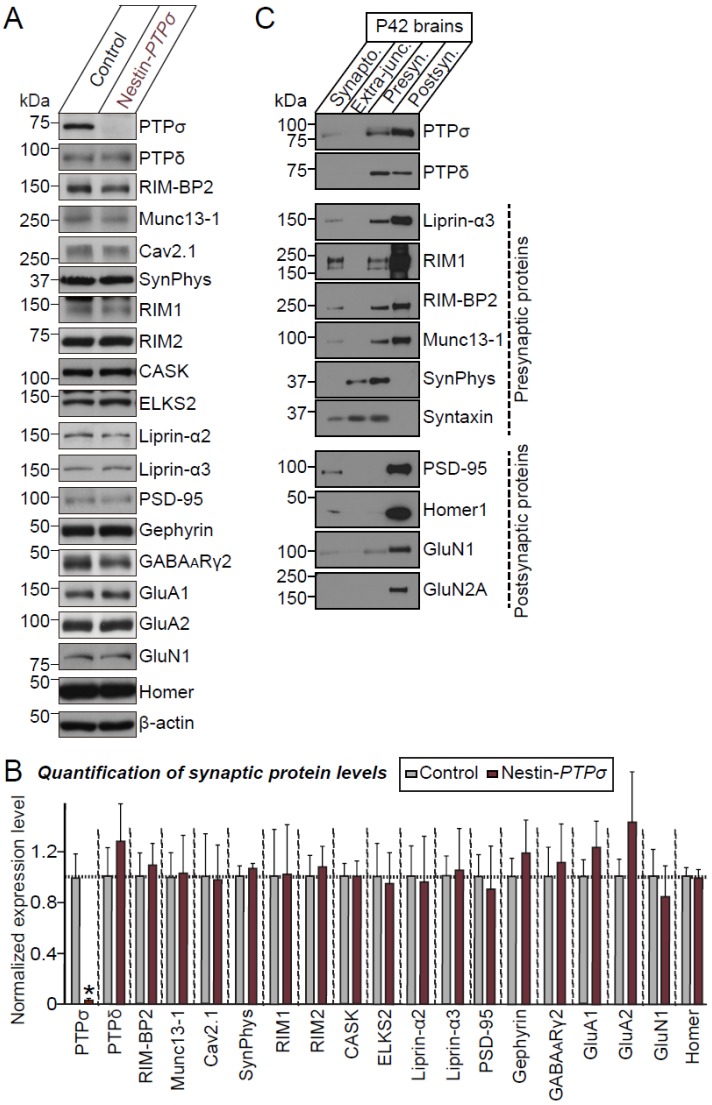

Supplemental Figure S5. Quantitative Immunoblot Analyses of PTPσ-deficient Mouse Brains. Related to *All Figures*.

(**A**) Representative images of immunoblot analysis using brain lysates from Nestin-*PTPσ* mice (n = 4 mice per group).

(**B**) Quantitative immunoblot analysis of PTPs, AZ proteins, and PSD proteins from control and Nestin-*PTPσ* mice. Data are means ± SEMs (n = 4 mice per group).

(**C**) Representative immunoblots of crude synaptosome (Synapto.), extrasynaptic junction (Extra-junc.), presynaptic (Presyn.), and postsynaptic (Postsyn.) fractions of adult mouse

brains. Both PTPσ and PTPδ were present at pre- and postsynaptic sites. Presynaptic active zone proteins and postsynaptic proteins were analyzed in parallel immunoblots.

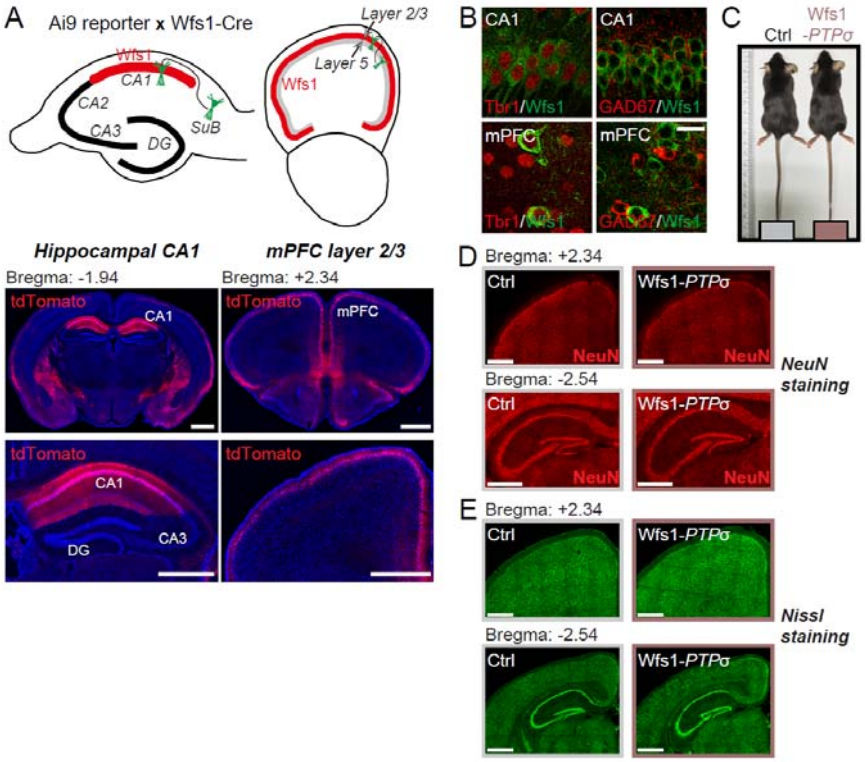

Supplemental Figure S6. Generation and Characterization of Wfs1-PTPσ KO Mice. Related to *Figures 4, 5, 6 & 7*.

(**A**) Schematic diagram (upper panel) and representative images (lower panel) of mice from the Wfs1-Cre driver line intercrossed with Ai9 reporter mice. tdTomato-positive neurons (red) in the hippocampal CA1 and layer II/III of the medial prefrontal cortex (mPFC) were detected by immunofluorescence analysis. Scale bar: 1 mm.

(**B**) Immunolocalization of Wfs1 protein (green) in mPFC and the hippocampal CA1 region of adult mice. Double immunofluorescence analysis for Tbr1 (red) and GAD67 (red) showed robust expression of Wfs1 in Tbr1-positive pyramidal neurons, but not in GAD67-positive inhibitory neurons. Scale bar: 20 μm.

(**C**) Images illustrating the body size of *PTPσ*$^{f/f}$ (Ctrl) and Wfs1-*PTPσ* littermates at 7 weeks of age. Body sizes of age- and sex-matched Ctrl and Wfs1-PTPσ mice were similar.

(**D**) Representative images of brain sections from *PTPσ*$^{f/f}$ (Ctrl) and Wfs1-*PTPσ* mice stained

with the neuronal marker NeuN (red). Scale bar: 1 mm.

(**E**) Representative images of brain sections from *PTPσ*$^{f/f}$ (Ctrl) and Wfs1-*PTPσ* mice stained with NeuroTrace™ 500/525 Green Fluorescent Nissl Stain solution (green). Scale bar: 1 mm.

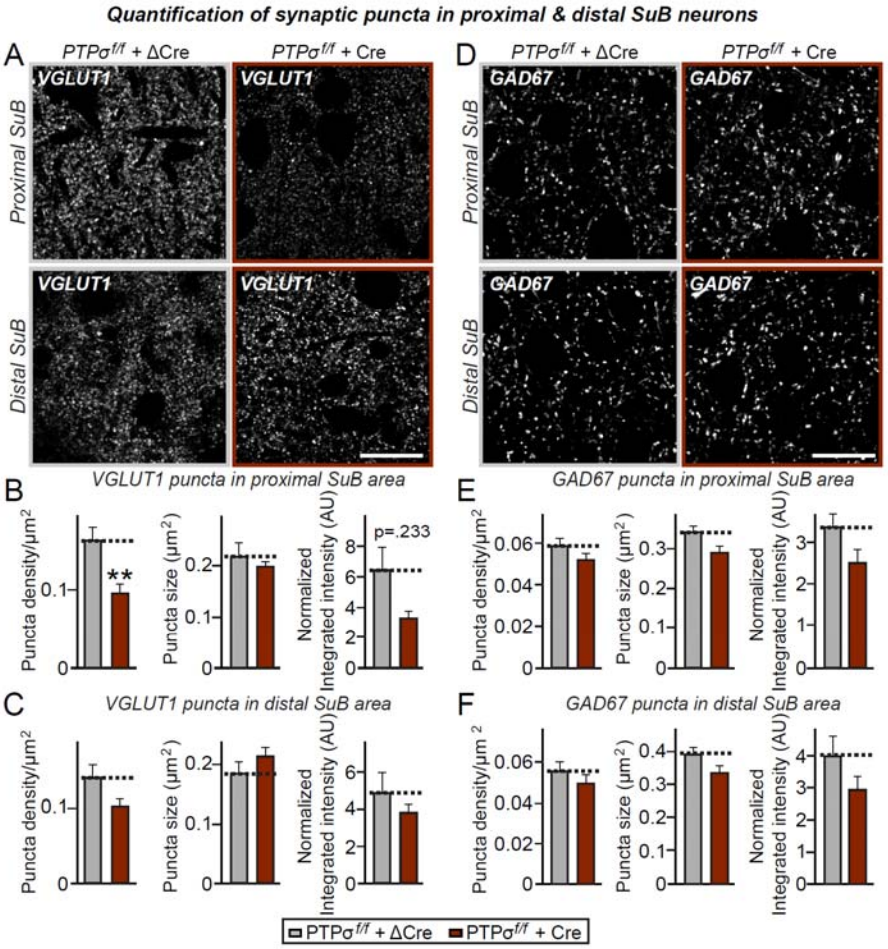

Supplemental Figure S7. Deletion of PTPσ from Hippocampal CA1 Specifically Decreases Innervation of Excitatory Synaptic Inputs on Subicular neurons. Related to *Figure 4*.

(**A, D**) Representative VGLUT1 (**A**) and GAD67 (**D**) positive immunofluorescence images of proximal and distal SuB of *PTPσ*$^{f/f}$ mice injected with AAV-ΔCre or AAV-Cre. Scale bar: 20 µm.

(**B, E**) Quantification of the density, size and integrated intensity of VGLUT1-positive (**B**) and GAD67-positive (**E**) synaptic puncta in proximal SuB. Data are means ± SEMs (n denotes the number of analyzed brain slices; 18–19 brain slices from 4 mice; $^{**}p < 0.01$; Mann Whitney U-test).

(**C, F**) Quantification of the density, size and integrated intensity of VGLUT1-positive (**C**) and GAD67-positive (**F**) synaptic puncta in distal SuB. Data are means ± SEMs (n denotes the number of analyzed brain slices; 18–19 brain slices from 4 mice; Mann Whitney U-test).

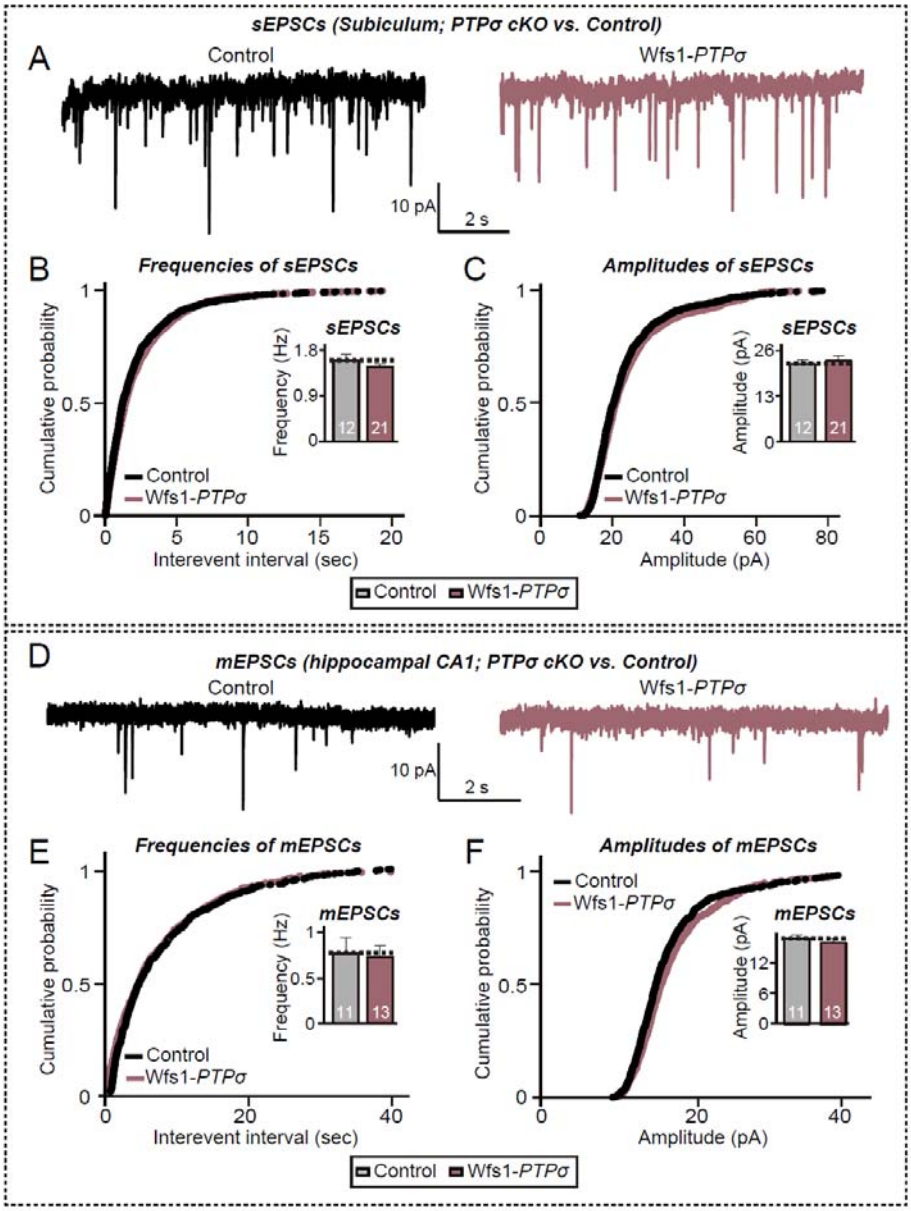

Supplemental Figure S8. Marginal Effect of Presynaptic Deletion of PTPσ on Excitatory and Inhibitory Synaptic Transmission in Pyramidal Neurons of Hippocampal Subiculum. Related to *Figure 4*.

(**A–C**) Representative sEPSC traces (**A**) recorded from SuB pyramidal neurons in acute SuB slices from littermate control and Wfs1-*PTPσ* mice, and cumulative distribution of sEPSC frequencies (**B**) and amplitudes (**C**). Insets show average sEPSC frequencies (**B**) and

amplitudes (**C**). Data are means ± SEMs (n denotes the number of analyzed neurons; Control, 12; and Wfs1-PTPσ, 21; two-tailed Student's t-tests).

(**D–F**) Representative mEPSC traces (**D**) recorded from CA1 pyramidal neurons in acute CA1 slices from littermate control and Wfs1-*PTPσ* mice, and cumulative distribution plots of mEPSC frequencies (**E**) and amplitudes (**F**). Insets show average mEPSC frequencies (**E**) and amplitudes (**F**). Data are means ± SEMs (n denotes the number of analyzed neurons; Control, 11; and Wfs1-*PTPσ*, 13; two-tailed Student's t-tests).

TRANSPARENT METHODS

KEY RESOURCES TABLE

REAGENT or RESOURCE	SOURCE	IDENTIFIER
Antibodies		
Mouse monoclonal Anti-PTPσ	MediMabs	Cat #MM-0020; RRID: AB_1808357
Mouse monoclonal Anti-GAD67	Millipore	Cat #MAB5406; RRID: AB_2278725
Rabbit polyclonal Anti-VGLUT1	Synaptic Systems	Cat #135 311; RRID: AB_887880
Guinea pig polyclonal Anti-VGLUT1	Millipore	Cat #AB5905; RRID: AB_2301751
Mouse monoclonal Anti-Gephyrin	Synaptic Systems	Cat #147 011; RRID: AB_887717
Mouse monoclonal Anti-PSD-95	NeuroMab	Cat #75-028; RRID: AB_2292909
Mouse monoclonal Anti-β-Actin	Santa Cruz Biotechnology	Cat #sc-47778; RRID: AB_626632
Rabbit polyclonal Anti-$GABA_AR\gamma 2$	Synaptic Systems	Cat #224 003; RRID: AB_2263066
Mouse monoclonal Anti-Gephyrin	Synaptic Systems	Cat #147 111; RRID: RRID: AB_887719
Mouse monoclonal Anti-Synaptophysin	Sigma-Aldrich	Cat #S5768; RRID: AB_477523
Mouse monoclonal Anti-CASK	NeuroMab	Cat #75-000; RRID: AB_2068730
Mouse monoclonal Anti-GluN1	Millipore	Cat #MAB363; RRID: AB_94946
Rabbit polyclonal Anti-Cav2.1	Synaptic systems	Cat #152 203; RRID: AB_2619841
Rabbit polyclonal anti-RIM1/2	Synaptic Systems	Cat #140 203; RRID: AB_887775
Rabbit polyclonal anti-Munc 13-1	Synaptic systems	Cat #126 103; RRID: AB_887733
Mouse monoclonal anti-ELKS	Sigma-Aldrich	Cat #E4531; AB_2100013
Rabbit polyclonal anti-GluA1	Kim et al., 2009	1193; RRID:AB_2722772
Rabbit polyclonal anti-GluA2	Kim et al., 2009	1195; RRID: AB_2722773
Rabbit polyclonal anti-pan-Shank	Kim et al., 2009	1172; RRID: AB_2810261
Rabbit polyclonal anti-Homer	Lie et al., 2016	1133; RRID: AB_2810985
Rabbit polyclonal anti-RIM-BP2	Synaptic systems	Cat #316 103; RRID: AB_2619739
Rabbit polyclonal anti-Liprin-α2	Han et al., 2018	RRID: AB_2810258
Rabbit polyclonal anti-Liprin-α3	Han et al., 2018	RRID: AB_2810259

Mouse monoclonal anti-Syntaxin	Synaptic systems	Cat # 110 011; RRID: AB_887844
Mouse monoclonal anti-Bassoon	Enzo Life Sciences	Cat # SAP7F407; RRID: AB_2313990
Rabbit polyclonal anti-GluN2A	Millipore	Cat # 07-632; RRID: AB_1121300
Mouse monoclonal anti-NeuN	Millipore	Cat # MAB377; RRID: AB_177621
Chicken polyclonal anti-Tbr1	Millipore	Cat # AB2261; RRID: AB_10615497
Rabbit polyclonal anti-Wfs1	Proteintech	Cat # 11558-1-AP RRID: AB_2216046
Rabbit polyclonal Anti-MAP2	Abcam	Cat # ab32454; RRID: AB_776174
Mouse monoclonal Anti-MAP2	Sigma-Aldrich	Cat # M1406; RRID: AB_477171
Cy3 conjugated Donkey Anti-Mouse	Jackson ImmunoResearch Laboratories	Cat #715-165-150; RRID: AB_2340813
Cy3 conjugated Donkey Anti-Rabbit	Jackson ImmunoResearch Laboratories	Cat #711-165-152; RRID: AB_2307443
Cy3 conjugated Donkey Anti-Guinea pig	Jackson ImmunoResearch Laboratories	Cat #706-165-148; RRID: AB_2340460
FITC conjugated Donkey Anti-Mouse	Jackson ImmunoResearch Laboratories	Cat #715-035-150; RRID: AB_2340770
FITC conjugated Donkey Anti-Rabbit	Jackson ImmunoResearch Laboratories	Cat #711-095-152; RRID: AB_2315776
FITC conjugated Donkey Anti-Chicken	Jackson ImmunoResearch Laboratories	Cat #703-095-155; RRID: AB_2340356
Chemicals, Peptides, and Recombinant Proteins		
Lipofectamine LTX Reagent with PLUS™ Reagent	ThermoFisher Scientific	Cat #15338100
Neurobasal medium	ThermoFisher Scientific	Cat #21103049
B-27 supplement (50X)	ThermoFisher Scientific	Cat #17504-044

Penicillin/Streptomycin	ThermoFisher Scientific	Cat #15140122
HBSS (Hanks' Balanced Salt Solution)	ThermoFisher	Cat #14065056
GlutaMax Supplement	ThermoFisher Scientific	Cat #35050061
Fetal Bovine Serum (FBS)	WELGENE	Cat #PK004-01
Sodium pyruvate	ThermoFisher Scientific	Cat #11360070
Poly-D-lysine hydrobromide	Sigma-Aldrich	Cat #P0899
Glutaraldehyde solution	Sigma-Aldrich	Cat #G5882
Sodium cacodylate trihydrate	Sigma-Aldrich	Cat #C4945
2,2,2-Tribromoethanol (Avertin)	Sigma	Cat #T48402
Ethanol	Millipore	Cat #1.00983.1011
Vectashield mounting medium	Vector Laboratories	Cat #H-1200
6-Cyano-7-nitroquinoxaline-2,3-dione (CNQX)	Sigma-Aldrich	Cat #C127
2,3-Dioxo-6-nitro-1,2,3,4-tetrahydrobenzo (NBQX)	Hello Bio	Cat #HB0443
Tetrodotoxin (TTX)	Tocris	Cat #1069
Bicuculline	Tocris	Cat #0130
Picrotoxin	Tocris	Cat #1128
QX-314	Tocris	Cat #1014
D-2-amino-5-phosphonovalerate (D-AP5)	Tocris	Cat #0106
Critical Commercial Assays		
ReverTra Ace-α Kit	Toyobo	Cat #FSQ-301
CalPhos Transfection Kit	Takara	Cat #631312
Experimental Models: Cell Lines		
HEK 293T cells	ATCC	Cat # CRL-3216
Cultured neurons (from mouse embryos)	N/A	N/A
Experimental Models: Organisms/Strains		

Mouse: *PTPσ* $^{f/f}$	KOMP Repository Collection	N/A
Mouse: *Wfs1-cre*	Kitamura et al., 2014	N/A
Mouse: *Nestin-cre*	The Jackson Laboratory	Cat #003771
Mouse: *Ai9 reporter*	The Jackson Laboratory	Cat #007909
Recombinant DNA		
pAAV-hSyn-ΔCre-GFP	Xu and Südhof, 2013	N/A
pAAV-hSyn-Cre-GFP	Xu and Südhof, 2013	N/A
FSW-ΔCre	Ko et al., 2011	N/A
FSW-Cre	Ko et al., 2011	N/A
L-313 PTPσ WT	Han et al., 2018	N/A
L-313 PTPσ C1157S	Han et al., 2018	N/A
L-313 PTPσ ΔD2	Han et al., 2018	N/A
pCAGG-VGLUT1-Venus	This study	N/A
Sequence-Based Reagents		
Ptprs mouse probe (for qRT-PCR)	This study	N/A
Ptprd mouse probe (for qRT-PCR)	This study	N/A
Ptprf mouse probe (for qRT-PCR)	This study	N/A
Software and Algorithms		
MetaMorph	Molecular Devices	https://www.moleculardevices.com
ImageJ	NIH	https://imagej.nih.gov/ij/
GraphPad Prism 8.0	GraphPad	https://www.graphpad.com
Clampfit 10.5	Molecular Devices	https://www.moleculardevices.com
AxoGraph	AxoGraph Scientific	https://axograph.com/

EXPERIMENTAL MODEL AND SUBJECT DETAILS

Cell Culture

HEK293T cells were cultured in Dulbecco's Modified Eagle's Medium (DMEM; WELGENE) supplemented with 10% fetal bovine serum (FBS; WELGENE) and 1% penicillin-streptomycin (Thermo Fisher) at 37°C in a humidified 5% CO_2 atmosphere. Cultured primary hippocampal neurons were prepared from embryonic day 17 (E17) *PTPσ*$^{f/f}$ mice.

Animals

The use and care of animals complied with the guidelines and protocols (DGIST-IACUC-17122104-01) for rodent experimentation approved by the Institutional Animal Care and Use Committee of DGIST under standard, temperature-controlled laboratory conditions. PTPσ conditional knockout mice were purchased from The KOMP Repository Collection (UC Davis, USA). Ai9 reporter mice were purchased from Jackson Research Laboratories (007909). Nestin-Cre (003771, Jackson Research Laboratories) mice were the gift of Dr. Albert Chen (DUKE-NUS, Singapore). Wfs1-Cre mice were the gift of Dr. Susumu Tonegawa (Massachusetts Institute of Technology, USA). Mice were kept on a 12:12 light/dark cycle (lights on at 9:00 am), and received water and food *ad libitum.* Floxed PTPσ (*PTPσ*$^{f/f}$) were generated by flanking exon 4 with loxP sites (See **Figs. S1** for details). Nestin-Cre driver line was crossed with *PTPσ*$^{f/f}$ mice to generate pan-neuronal PTPσ knockout. Wfs1-Cre driver line was crossed with PTPσ$^{f/f}$ mice to generate mPFC and CA1-specific knockout. Mice were maintained in the C57BL/6N background. Breeding cages are maintained by crossing male PTPσ$^{f/f}$ with female PTPσ$^{f/+}$::Nestin HET (generated by crossing PTPσ$^{f/WT}$ with heterozygous Nestin-Cre transgenic mice), or male *PTPσ*$^{f/f}$ with female *PTPσ*$^{f/f}$::Wfs1 HET (generated by crossing *PTPσ*$^{f/f}$ with heterozygous Wfs1-Cre transgenic mice) mice. All experimental procedures were performed on male mice, using

littermate control without Cre expression.

METHOD DETAILS

Construction of Expression Vectors. *1. PTPσ rescue constructs.* The lentiviral PTPσ rescue vectors were previously described (Han et al., 2018). *2. Others*. The plasmids pAAV-hSyn-ΔCre-GFP and pAAV-hSyn-Cre-GFP were from Dr. Thomas C. Südhof (Stanford University, Palo Alto, CA, USA); FSW-ΔCre and FSW-Cre were from Dr. Pascal S. Kaeser (Harvard University, Cambridge, MA, USA); and pCAGG-VGLUT1-Venus was from Dr. Franck Polluex (Columbia University, New York, NY, USA).

Antibodies. Commercially obtained antibodies included: mouse monoclonal anti-GAD67 (clone 1G10.2; Millipore; RRID: AB_2278725), guinea pig polyclonal anti-VGLUT1 (Millipore; RRID: AB_2301751), rabbit polyclonal anti-VGLUT1 (Synaptic Systems; RRID: AB_887880), rabbit polyclonal anti-$GABA_AR\gamma2$ (Synaptic Systems; RRID: AB_2263066), mouse monoclonal anti-PSD-95 (clone K28/43; Neuromab; RRID: AB_2292909), mouse monoclonal anti-PTPσ (clone 17G7.2; MediMabs; RRID: AB_1808357), mouse monoclonal anti-CASK (clone K56A/50; NeuroMab; RRID: AB_2068730), mouse monoclonal anti-HA (clone 16B12; BioLegend; RRID: AB_2565006); mouse monoclonal anti-Bassoon (clone SAP7F407; Enzo Life Sciences; RRID: AB_2313990), mouse monoclonal anti-Syntaxin (clone SAP7F407; Enzo Life Sciences; RRID: AB_887844), mouse monoclonal anti-NeuN (clone A60; Millipore; RRID: AB_177621), chicken polyclonal anti-Tbr1 (Millipore; RRID: AB_177621), rabbit polyclonal anti-Wfs1 (Proteintech; AB_2216046), goat polyclonal anti-GFP (Rockland; AB_218182), rabbit polyclonal anti-GluN2A (Millipore; AB_11213002), rabbit polyclonal anti-Munc13-1 (Synaptic Systems; RRID: AB_887733), rabbit polyclonal anti-RIM-BP2 (Synaptic Systems; RRID: AB_2619739), rabbit

polyclonal anti-RIM1/2 (Synaptic Systems; RRID: AB_887775), mouse monoclonal anti-ELKS (Sigma-Aldrich; RRID: AB_2100013), mouse monoclonal anti-Synaptophysin (clone SVP-38; Sigma-Aldrich; RRID: AB_477523), mouse monoclonal anti-MAP2 (clone AP-20; Sigma-Aldrich; RRID: AB_477171), rabbit polyclonal anti-MAP2 (Abcam; RRID: AB_776174), mouse monoclonal anti-β-actin (clone C4; Santa Cruz Biotechnology; RRID: AB_626632), mouse monoclonal GluN1 (clone 54.1; Millipore; RRID: AB_94946), rabbit polyclonal Cav2.1 (Synaptic Systems; RRID: AB_2619841), and mouse monoclonal anti-Gephyrin (clone 3B11; Synaptic Systems; RRID: AB_887717). Rabbit polyclonal anti-liprin-α2 (RRID:AB_2810258) and rabbit polyclonal anti-liprin-α3 (RRID:AB_2810259) antibodies were gifts of Dr. Susanne Schoch-McGovern (Bonn, Germany); rabbit polyclonal anti-pan-Shank (1172; RRID: AB_2810261), rabbit polyclonal anti-GluA1 (1193; RRID: AB_2722772), rabbit polyclonal anti-GluA2 (1195; RRID: AB_2722773), and rabbit polyclonal anti-Homer1 antibodies (1133; RRID: AB_2810985) were the gifts of Dr. Eunjoon Kim (KAIST, Korea).

Chemicals. 6-Cyano-7-nitroquinoxaline-2,3-dione (CNQX) was obtained from Sigma-Aldrich (Cat No. C127). Tetrodotoxin (TTX; Cat No. 1069); picrotoxin (Cat No. 1128), QX-314 (Cat No. 1014); and D-2-amino-5-phosphonovalerate (D-AP5; Cat No. 0106) were purchased from Tocris.

Neuron Culture, Transfections, Imaging, and Quantitation. Hippocampal and cortical mouse neuron cultures were prepared from embryonic day 17 (E1) mouse embryos, as described previously (Ko et al., 2011). Mouse cultured neurons were seeded onto coverslips coated with poly-D-lysine (Sigma-Aldrich), and grown in Neurobasal medium supplemented with B-27 (Thermo Fisher), 0.5% FBS (WELGENE), 0.5 mM GlutaMAX (Thermo Fisher), and sodium pyruvate (Thermo Fisher). Cultured neurons (mostly excitatory neurons) were infected with lentiviruses at DIV3–4. For

immunocytochemistry, cultured neurons were fixed with 4% paraformaldehyde/4% sucrose in PBS for 10–30 min at 4°C, and permeabilized with 0.2% Triton X-100 in PBS for 10–30 min at 4°C. Neurons were blocked with 3% horse serum/0.1% BSA in PBS for 15 min at room temperature and incubated with primary and secondary antibodies in blocking solution for 70 min at room temperature. The primary antibodies were used in these experiments included anti-VGLUT1 (Synaptic Systems; 1:700), anti-GAD67 (Millipore; 1:100), anti-$GABA_AR\gamma2$ (Synaptic Systems; 1:500), anti-GluA1 (1193; 1:200), anti-Gephyrin (Synaptic Systems; 1:100), and anti-pan-Shank (1172; 1:200). Images of randomly selected neurons were acquired using a confocal microscope (LSM800, Carl Zeiss) with a 63 × objective lens; all image settings were kept constant during image acquisition. Z-stack images obtained by confocal microscopy were converted to maximal projections, and puncta size and the density of the indicated presynaptic marker proteins were analyzed in a blinded manner using MetaMorph software (Molecular Devices Corp.).

Production of Lentiviruses. Lentiviruses were produced by transfecting HEK293T cells with three plasmids—lentivirus vectors, psPAX2, and pMD2.G—at a 2:2:1 ratio. After 72 h, lentiviruses were harvested by collecting the media as previously described (Han et al., 2018; Hsia et al., 2014).

Production of Adeno-associated Viruses. HEK293T cells were co-transfected with the indicated AAV vectors, pHelper and AAV1.0 (serotype 2/9) capsids vectors. After 72 hours, the transfected HEK293T cells were collected, and resuspended in PBS, and lysed by subjecting them to four freeze-thaw cycles in an ethanol/dry ice bath (7 minutes each) and a 37°C water bath (5 min). The lysates were centrifuged and the supernatants were mixed with 40% polyethylene glycol and 2.5 M NaCl and centrifuged at 2000 × g for 30 min. The cell pellets were resuspended in HEPES buffer (20 mM HEPES, 115 mM NaCl, 1.2 mM $CaCl_2$, 1.2 mM $MgCl_2$, and 2.4 mM KH_2PO_4, pH 8.0) to which was added an equal volume of chloroform. The mixture was centrifuged at 400 × g for 5 min and concentrated

three times with a Centriprep centrifugal filter (Cat. 4310, Millipore) at 1,220 × g (20 min each) and an Amicon Ultra centrifugal filter (Cat. UFC500396, Millipore) at 16,000 × g for 30 min. AAVs were titered by treating 1 µl of concentrated, filter-sterilized AAVs with 1 µl of DNase I (AMPD1; Sigma) for 30 min at 37 °C to eliminate any contaminating plasmid DNA. After treatment with 1 µl of stop solution (50 mM ethylenediaminetetraacetic acid) for 10 min at 65 °C, 10 µg of protease K (Cat. P2308; Sigma) was added and the sample was incubated for 1 h at 50°C. Reactions were stopped by heat inactivation at 95 °C for 20 min. The final virus titer was quantified by qRT-PCR. Empty AAV vector was used to generate a standard curve for qRT-PCRs targeting *GFP* sequences.

qRT-PCRs. Cultured rat cortical neurons were infected with recombinant lentiviruses at DIV4 and harvested at DIV13 for qRT-PCR using SYBR green qPCR master mix (TaKaRa). Total RNA was extracted from mouse cortical neurons using TRIzol reagent (Invitrogen) according to the manufacturer's protocol. Briefly, cells in each well of a 12-well plate of cultured neurons were harvested and incubated with 500 µl TRIzol reagent at room temperature for 5 minutes. After phenol-chloroform extraction, RNA in the upper aqueous phase was precipitated. cDNA was synthesized from 500 ng of RNA by reverse transcription using a ReverTra Ace-α kit (Toyobo). Quantitative PCR was performed on a CFX96 Touch Real-Time PCR system BioRad) using 0.5 µl of cDNA. The ubiquitously expressed β-actin was used as an endogenous control. The sequences of the primer pairs used were: mouse *Ptprs*, 5'-ATCAGAGAGCCCAAGGATCA-3' (forward) and 5'-GCCACACACTCGTACACGTT-3' (reverse); mouse *Ptprd*, 5'-CTCCTTGATCCCCATCTCTG–3' (forward) and 5'-CAG GGCAGCCACTAAACTTC-3' (reverse); and mouse *Ptprf*, 5'- CCCGATGGCTGAGTACAACA-3' (forward) and 5'-CATCCCGGGCGTCTGTGA-3' (reverse).

Electron Microscopy. E17 embryonic hippocampi of *PTPσ*$^{f/f}$ mice were seeded onto 18 mm coverslips at densities of 40,000 cells/well. The neurons were infected with lentiviral vectors expressing ΔCre or

Cre at DIV4. At DIV14, cultured neurons were fixed in 2% glutaraldehyde, 0.1 M Na-cacodylate buffer, pH 7.4, for 1 h at room temperature and overnight at 4°C. The cells were post-fixed in 0.5% OsO4 (osmium tetroxide), 0.8% K ferricyanide at room temperature for 60 min. All specimens were stained *en bloc* with 2% aqueous uranyl acetate for 30 min, dehydrated in a graded ethanol series up to 100%, embedded in Embed 812 resin (Electron Microscopy Science, PA), and polymerized overnight in a 60 °C oven. Thin sections (50–60 nm) were cut with a Leica ultramicrotome and post-stained with uranyl acetate and lead citrate. Sample grids were examined using a FEI Tecnai BioTWIN transmission electron microscope running at accelerating voltage of 80 kV. Images were recorded with a Morada CCD camera and iTEM (Olympus) software. This protocol allowed the unambiguous staining of membranes of synaptic vesicles as well as of pre- and post-synaptic compartments, resulting in accurate measurements of the nanoscale organization of the synaptic vesicles within nerve endings. To analyze synapse ultrastructure, the lengths of active zone and PSD, tethered vesicles, the membrane proximal vesicles, and total vesicle numbers were quantified using MetaMorph software (Molecular Devices Corp.). The numbers of total vesicles and docked vesicles were counted manually, and the distances from the active zone and the PSD to the vesicle center were measured. Vesicles located below 200 nm were considered membrane-proximal vesicles.

RNAscope Analyses. RNAscope analyses of mouse brains were performed using RNAscope® Fluorescent Multiplex Assay kits (Advanced Cell Diagnostics) according to the manufacturer's direction. Briefly, within 5 min of dissection, mouse brains were immersed in cryo-embedding medium and frozen on dry ice. Brain tissue was sliced into 20 µm-thick coronal sections using a cryotome (Model CM-3050-S; Leica Biosystems), mounted, and dried at –20°C for 10 min. Tissue samples were fixed with 4% formaldehyde for 15 minutes at 4°C and dehydrated by incubation at room temperatures (RT) in 50% EtOH for 5 min, in 70% EtOH for 5 min, and twice 100% EtOH for 5 min. The fixed samples were treated with protease IV for 30 min at RT and

washed twice with 1X PBS. To detect RNA, the sections were incubated in different amplifier solutions in a HybEZ hybridization oven (Advanced Cell Diagnostics) at 40°C. Three synthetic oligonucleotides complementary to nucleotide residues 1051–1947 of Mm–*Ptprs*–C1, 1329–2486 of Mm-*Ptprd*–C1 and Mm-*Ptprd*–C2, and 4001–5386 of Mm–*Ptprf*-C3 (Advanced Cell Diagnostics) were labeled by conjugation to Alexa Fluor 488, Altto 550 and Altto 647, and the labeled probe mixtures were hybridized by tissue samples by incubating them with slide-mounted sections for 2 hours at 40°C. Nonspecifically hybridized probes were removed by washing the sections three times for 2 minutes each with 1X wash buffer at RT, followed by incubations at 40°C with Amplifier 1-FL for 30 minutes, Amplifier 2-FL for 15 minutes, Amplifier 3-FL for 30 minutes, and Amplifier 4 Alt B-FL for 15 minutes. Each amplifier was removed by washing twice in 1X wash buffer at RT. The fluorescence images were acquired using a LSM 800 microscope (Carl Zeiss).

Stereotaxic Surgery and Virus Injections. 6–7-week-old mice were anesthetized by intraperitoneal injection of 2% 2,2,2-tribromoethanol (Sigma), dissolved in saline, and secured in a stereotaxic apparatus. Viral solutions were injected using a Nanoliter 2010 Injector (World Precision Instruments), including a NanoFil syringe and 33 gauge needle, at a flow rate of 50 nl/min (injected volume, 500 nl). The coordinates used for stereotaxic injections targeting the ventral hippocampal CA1 were, relative to the bregma, anteroposterior (AP) -3.1 mm; medial–lateral (ML), ± 3.2 mm; and dorsal–ventral (DV), -2.5 mm. Immunohistochemical analyses were performed 3 weeks later.

Immunohistochemistry. Male mice aged 8–10-weeks were anesthetized and immediately perfused, first with PBS for 5 minutes and then with 4% paraformaldehyde for 5 minutes. Their brains were removed, fixed overnight in 4% paraformaldehyde, incubated overnight in 30% sucrose (in PBS), and

sliced into 35-µm-thick coronal sections using a cryotome (Model CM-3050-S; Leica Biosystems). The sections were permeabilized in PBS containing 0.5% Triton X-100 for 1 h and blocked in PBS containing 5% bovine serum albumen and 5% horse serum for 1 minutes. The brain sections were incubated overnight with primary antibodies for overnight at 4 °C. The following primary antibodies were used: anti-VGLUT1 (1:200), anti-GAD67 (1:100). The brain sections were washed three times with PBS and incubated with the appropriate Cy3-conjugated secondary antibodies (Jackson ImmunoResearch) for 2 hours at RT. After three washes with PBS, the sections were counterstained with DAPI (4',6-diamidino-2-phenylinodole) and mounted onto glass slides (Superfrost Plus; Fisher Scientific) with Vectashield mounting medium (H-1200; Vector Laboratories).

In Vitro **and** ***Ex Vivo*** **Electrophysiology.** *1. Electrophysiology of Primary Cultured Neurons.* Hippocampal neurons obtained from PTPσ cKO mice were infected on DIV4 with lentiviruses encoding Cre-EGFP or dCre-EGFP, followed by analysis at DIV13-16. Pipettes were pulled from borosilicate glass (o.d. 1.5 mm, i.d. 0.86 mm; Sutter Instrument), using a Model P-97 pipette puller (Sutter Instrument). The resistance of pipettes filled with internal solution varied between 3-6 MΩ. The internal solution (in mM) contained 145 CsCl, 5 NaCl, 10 HEPES, 10 EGTA, 0.3 Na-GTP, and 4 Mg-ATP with pH adjusted to 7.2–7.4 with CsOH, and an osmolarity of 290–295 mOsmol/L. The external solution (in mM) consisted of 130 NaCl, 4 KCl, 2 $CaCl_2$, 1 $MgCl_2$, 10 HEPES, and 10 D-glucose with pH adjusted to 7.2–7.4 with NaOH, and an osmolarity of 300–305 mOsmol/L. Whole-cell configuration was generated at RT using MPC-200 manipulators (Sutter Instrument) and a Multiclamp 700B amplifier (Molecular Devices). mEPSCs, mIPSCs, and sucrose EPSCs were recorded at a holding potential of -70 mV. For sucrose puffing, 500 mM sucrose was applied directly on the dendritic field of the patched neurons at a puff pressure of 6–8 psi using a PV-820 Pneumatic Picopump system (World Precision Instruments). Receptor-mediated synaptic responses were pharmacologically isolated by applying drug

combinations of 50 μM picrotoxin, 10 μM CNQX, 50 μM D-APV and/or 1 μM tetrodotoxin. Synaptic currents were analyzed offline using Clampfit 10.5 (Molecular Devices) software. *2. Acute Slice Electrophysiology*. Transverse hippocampal formation (300 μm) were prepared from 10–12-week-old male mice, as described (Noh et al., 2019). The mice were anesthetized with isoflurane and decapitated, and their brains were rapidly removed and placed in ice-cold, oxygenated (95% O_2/5% CO_2), low-Ca^{2+}/high-Mg^{2+} dissection buffer (in mM) containing 5 KCl, 1.23 NaH_2PO_4, 26 $NaHCO_3$, 10 dextrose, 0.5 $CaCl_2$, 10 $MgCl_2$, and 212.7 sucrose. Slices were transferred to a holding chamber in an incubator containing oxygenated (95% O_2/5% CO_2) artificial cerebrospinal fluid (ACSF in mM) containing 124 NaCl, 5 KCl, 1.23 NaH_2PO_4, 2.5 $CaCl_2$, 1.5 $MgCl_2$, 26 $NaHCO_3$, and 10 dextrose at 28–30°C for at least 1 h before recording. After > 1 h incubation in ACSF, slices were transferred to a recording chamber with continuous perfusion (2 ml/min) by ACSF oxygenated with 95% O_2/5% CO_2 at 23–25°C. All recordings were performed on pyramidal neurons in the subiculum or hippocampal CA1 area identified by their size and morphology. Patch pipettes (4–6 MΩ) were filled with a solution (in mM) containing 130 Cs-$MeSO_4$, 0.5 EGTA, 5 TEA-Cl, 8 NaCl, 10 HEPES, 1 QX-314, 4 ATP-Mg, 0.4 GTP-Na, and 10 phosphocreatine-Na_2 to record mEPSCs and AMPA/NMDA ratio; 135 K-gluconate, 8 NaCl, 10 HEPES, 2 ATP-Na and 0.2 GTP-Na to record sEPSCs and eEPSC-PPRs with pH 7.4 and an osmolarity of 280–290 mOsmol/L. The extracellular recording solution consisted of ACSF supplemented with picrotoxin (100 μM) for sEPSCs, and with TTX (1 μM), DL-AP5 (50 μM), and picrotoxin (100 μM) for measuring mEPSCs. Evoked synaptic responses were elicited by stimulation (0.2 ms current pulses) using a concentric bipolar electrode placed 200–300 mm in front of postsynaptic pyramidal neurons at intensities that produced 40–50% of the maximal EPSC amplitude. Recordings were obtained using a Multiclamp 700B amplifier (Molecular Devices) under visual control with differential interference contrast illumination on an upright microscope (BX51WI; Olympus). Data were acquired and analyzed using pClamp 10.7

(Molecular Devices). Signals were filtered at 3 kHz and digitized at 10 kHz with DigiData 1550 (Molecular Devices).

QUANTIFICATION AND STATISTICAL ANALYSIS

Data Analysis and Statistics. All data are expressed as means ± SEM. All experiments were repeated using at least three independent cultures, and data were statistically evaluated using a Mann-Whitney *U* test, analysis of variance (ANOVA) followed by Tukey's *post hoc* test, Kruskal-Wallis test (one-way ANOVA on ranks), paired two-tailed t-test (for electrophysiology experiments), or one-way ANOVA with Bonferroni's *post hoc* test (for behavior experiments), as appropriate. Prism8 (GraphPad Software) was used for analysis of data and preparation of bar graphs. *P* values < 0.05 were considered statistically significant (individual *p* values are presented in figure legends).

SUPPLEMENTAL REFERENCES

Han, K.A., Ko, J.S., Pramanik, G., Kim, J.Y., Tabuchi, K., Um, J.W., and Ko, J. (2018). PTPsigma Drives Excitatory Presynaptic Assembly via Various Extracellular and Intracellular Mechanisms. J. Neurosci. 38, 6700-6721.

Hsia, H.E., Kumar, R., Luca, R., Takeda, M., Courchet, J., Nakashima, J., Wu, S., Goebbels, S., An, W., Eickholt, B.J.*, et al.* (2014). Ubiquitin E3 ligase Nedd4-1 acts as a downstream target of PI3K/PTEN-mTORC1 signaling to promote neurite growth. Proc. Natl. Acad. Sci. U S A 111, 13205-13210.

Kim, M.H., Choi, J., Yang, J., Chung, W., Kim, J.H., Paik, S.K., Kim, K., Han, S., Won, H., Bae, Y.S.*, et al.* (2009). Enhanced NMDA receptor-mediated synaptic transmission, enhanced long-term potentiation, and impaired learning and memory in mice lacking IRSp53. J. Neurosci. 29, 1586-1595.

Kitamura, T., Pignatelli, M., Suh, J., Kohara, K., Yoshiki, A., Abe, K., and Tonegawa, S. (2014). Island cells control temporal association memory. Science 343, 896-901.

Ko, J., Soler-Llavina, G.J., Fuccillo, M.V., Malenka, R.C., and Südhof, T.C. (2011). Neuroligins/LRRTMs prevent activity- and Ca2+/calmodulin-dependent synapse elimination in cultured neurons. J. Cell Biol. 194, 323-334.

Lie, E., Ko, J.S., Choi, S.Y., Roh, J.D., Cho, Y.S., Noh, R., Kim, D., Li, Y., Kang, H., Choi, T.Y.*, et al.* (2016). SALM4 suppresses excitatory synapse development by cis-inhibiting trans-synaptic SALM3-LAR adhesion. Nat. Commun. 7, 12328.

Noh, K., Lee, H., Choi, T.Y., Joo, Y., Kim, S.J., Kim, H., Kim, J.Y., Jahng, J.W., Lee, S., Choi, S.Y., and Lee, S.J. (2019). Negr1 controls adult hippocampal neurogenesis and affective behaviors. Mol. Psychiatry 24, 1189-1205.

Xu, W., and Südhof, T.C. (2013). A neural circuit for memory specificity and generalization. Science 339, 1290-1295.